High Energy Nuclear Interactions in Lead*

FRITZ E. FROEHLICH, ERICH M. HARTH,† AND KURT SITTE
Department of Physics, Syracuse University, Syracuse, New York
(Received March 12, 1952)

In an attempt to study details of cosmic-ray nuclear interactions a large cloud chamber containing eight ½-inch lead plates was operated in conjunction with a 134-counter hodoscope placed directly below the chamber, at Echo Lake, Colorado (altitude, 3260 m) and at Syracuse, New York (altitude, 220 m). Showers produced in the chamber were detected by counter trays above and below the chamber, producing a masterpulse which triggered both the chamber and the hodoscope. It was then possible to follow in the hodoscope the further development of the nuclear cascade started in the chamber, and to study for each event both the individual features of the interaction from the cloud-chamber photograph, and, at least statistically, the properties of the secondaries from the hodoscope record. In particular, the "integral path length" of the nuclear cascade in the approximately 600 g/cm² lead absorber of the hodoscope, is a measure of the energy of the primary particle. It is concluded that most of the primaries recorded had energies between 1 and 10 Bev. The analysis of about 400 shower pictures shows no appreciable difference between the events observed at the two locations. Both show a variation of the primary mean free path from about 190 g/cm² to 160 g/cm² over the energy interval covered. The statistics are not good enough to decide whether the mean free path of the secondaries also varies with the primary energy; a mean value of 250 g/cm² was observed. The ratio of the number of charged mesons to the number of protons increases from about 0.4 to 2.1, while the ratio of neutral to charged mesons is found to be 0.55±0.1 for low multiplicities, and its lower limit for higher multiplicities is 0.36±0.1. A distribution function was derived for the total shower multiplicities as a function of the primary energy. For low primary energies, small multiplicities are favored; but with increasing primary energy the distribution function becomes rather flat. The primary energy spectrum found agrees satisfactorily with the observations of other authors.

I. INTRODUCTION

HIGH energy nuclear interactions in lead have been studied extensively, both in cloud-chamber investigations,[1–7] and with counter arrangements.[8–11] Qualitatively, the basic processes involved in these events have been recognized: the multiplicative character of the nuclear "cascades" has been established, as well as the identity of most of the particles that make up the interacting, or N-component. The mean free path of the particles initiating the nuclear interactions in lead has been found to increase slightly from the "geometrical" value of 160 g/cm² at the high energies to values around 200–250 g/cm² at the lower energies, the mean free path of the shower secondaries being not very different from that of the primaries. The collisions are predominantly elastic for primary energies in the neighborhood of the threshold for meson production, and become increasingly inelastic for higher energies, the degree of inelasticity being essentially constant above a few Bev. A component of neutral mesons is by now fairly well established, their number being comparable to the number of charged mesons produced.

Apart from these descriptive features, however, the physical picture of these interactions is still rather obscure. In particular, the information thus far collected from experiments is still inadequate to bring to a test the various theories on fast collisions.[12–15] This is partly due to the slow rate of penetrating showers at sea level, or even mountain altitudes, and the resulting poor statistics of most investigations, and partly to the limited scope of information that can be derived from any one experiment.

This last fault arises from a very simple dilemma: cloud-chamber studies are well suited for an analysis of the secondary particles, and give perhaps the most unambiguous picture of the general features of a nucleonic event. They furnish, however, very little information on the energy of the primary particle. The two methods used,—the single shower producing layer in a chamber that is immersed in a magnetic field,[1] and the multiple plate chamber in which the primary energies are determined from scattering measurements,[7] are in general good only up to about 2 Bev and will not enable one to differentiate between the more energetic primaries. Counter experiments, on the other hand, can do somewhat better with respect to energy determination, but are by far inferior as a means of studying the structure and composition of showers.

In order to overcome some of these difficulties, an experiment was designed that would permit the simul-

* Supported in part by the AEC. Part of this paper was submitted by E. M. H. as a Ph.D. thesis at Syracuse University.
† Now at the Naval Research Laboratory, Washington, D. C.
[1] G. D. Rochester, Proc. Phys. Soc. (London) **A187**, 464 (1946); G. D. Rochester and C. C. Butler, Proc. Phys. Soc. (London) **A61**, 535 (1948).
[2] W. B. Fretter, Phys. Rev. **73**, 41 (1948); **76**, 511 (1949).
[3] H. S. Bridge and W. E. Hazen, Phys. Rev. **74**, 579 (1948).
[4] C. Y. Chao, Phys. Rev. **75**, 581 (1948).
[5] Lovati, Mura, Salvini, and Tagliaferri, Phys. Rev. **77**, 284 (1950).
[6] W. S. Brown and A. S. McKay, Phys. Rev. **77**, 342 (1950).
[7] B. P. Gregory and J. H. Tinlot, Phys. Rev. **81**, 667 and 675 (1951).
[8] G. Cocconi, Phys. Rev. **75**, 1974 (1949).
[9] W. D. Walker, Phys. Rev. **77**, 686 (1950).
[10] K. Sitte, Phys. Rev. **78**, 714 (1950).
[11] Greisen, Walker, and Walker, Phys. Rev. **80**, 535 and 546 (1950).
[12] W. Heisenberg, Z. Physik **113**, 61 (1939); **126**, 569 (1949).
[13] Lewis, Oppenheimer, and Wouthuysen, Phys. Rev. **73**, 127 (1948).
[14] W. Heitler and L. Jánossy, Proc. Roy. Soc. (London) **A62**, 374 (1949).
[15] E. Fermi, Prog. Theoret. Phys. **5**, 570 (1950); Phys. Rev. **81**, 683 (1951).

taneous determination of the energy of the primary as well as the structural details of the nuclear events. For this purpose a large multiple plate cloud chamber was operated in conjunction with a counter hodoscope. The hodoscope was to contain enough absorbing material to make possible an energy estimate based on the absorption of the nuclear cascade and the characteristic features of the interaction as shown in the cloud-chamber record. Primary energies up to about 10 Bev were to be determined in this way. With such an arrangement one is now in a position to compare the various features of nuclear events, such as their multiplicity, the number of charged and neutral mesons per event, and the energy absorbed in the electronic component, with a physically significant "abscissa,"—the energy of the initiating particle.

II. DETAILS OF THE EXPERIMENTAL ARRANGEMENT

(1) Cloud Chamber and Hodoscope

A cloud chamber of dimensions 24 in.×24 in.×10 in., with an illuminated depth of about 7 in., was fitted with eight $\frac{1}{2}$-inch lead plates. It was filled with argon, and operated at a few centimeters Hg above atmospheric pressure in its expanded state. Stereoscopic photographs were taken on 70-mm film with a single Beattie-Varitron camera, using a mirror system that gave an effective angular separation of about 15°. High expansion speed was achieved by using a pneumatic-relay type of expansion valve which controlled an opening of about 200 cm².

The hodoscope consisted of 134 counters arranged in five trays (A to E) as shown in the schematic diagram Fig. 1. Tray A contained twenty 1 in.×12 in. counters, tray B twenty-four counters of the same size. The counters used in trays C to E were 1 in.×16 in., numbering twenty-eight, thirty, and thirty-two, respectively. Absorbers of 4-in. Pb and $\frac{1}{4}$-in. Fe were placed on top of A and between the trays, making a total of 580 g/cm² Pb plus 24 g/cm² Fe. All trays were shielded against side showers by 6-in. Pb.

The cathode follower outputs of all hodoscope counters were fed into coincidence with the master-pulse (defined in the next paragraph). Thyratron triggering circuits, mounted on interchangeable panels, controlled the 134 neon bulbs which were photographed by a separate camera. The operation of the circuits could be tested at all critical points while the experiment was running, and a number of reserve panels were prepared to minimize losses in operating time.

The proper correlation of the cloud chamber and hodoscope pictures was assured by a threefold check: both photographs show synchronized clocks and two registers, one operated from the chamber triggering pulse and the other from the hodoscope camera circuit. In addition, a neon indicator bulb showed on the cloud-chamber picture whenever the hodoscope was triggered,

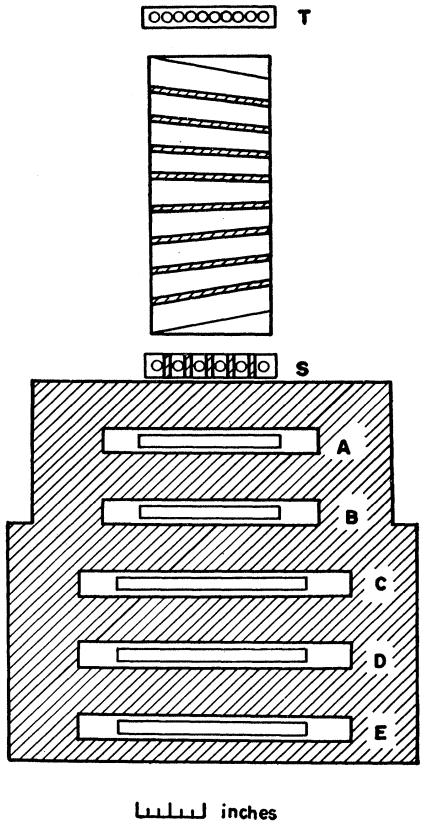

FIG. 1. The experimental arrangement. "Top tray" T: ten counters 1 in.×20 in.; "Shower tray" S: six counters 1 in.×20 in. with $\frac{3}{4}$ in. lead spacers; hodoscope trays A: twenty counters 1 in.×12 in.; B: twenty-four counters 1 in.×12 in.; C: twenty-eight counters 1 in.×16 in., D: thirty counters 1 in.×16 in.; E: thirty-two counters 1 in.×16 in.

and a corresponding one showed on the hodoscope panel whenever the chamber was expanded.

(2) The Triggering System

The nuclear interactions taking place in the cloud chamber were selected by the two trays of counters, T and S, shown in Fig. 1. Here, the "top" tray, T, consists of ten 1 in.×20 in. counters with two subgroups T_1 and T_2 of five not neighboring counters each, connected in parallel. The "shower" tray, S, containing six 1 in.×20 in. counters was similarly divided into the subgroups S_1 and S_2. The counters in this tray were separated from one another by $\frac{3}{4}$-in. strips of lead. A masterpulse was fed to both the cloud chamber and the hodoscope, whenever a discharge in one, and only one, of the subgroups in T was accompanied by a discharge in both of the subgroups in S. With these requirements low energy nuclear events were accepted with relatively high efficiency, while μ-meson knock-on events were mostly eliminated by the $\frac{3}{4}$ in. lead strips in the S tray. The anticoincidences between T_1 and T_2 provide a strong bias against large air showers, while air showers of low particle density may, on occasion,

miss one-half of T and give rise to a masterpulse. An estimate of the number of air showers among the genuine masterpulses was obtained by operating during part of the experiment an unshielded extension tray located at about 2 m from the chamber, and consisting of six 2 in.×24 in. counters, arranged in two subgroups. Two neon bulbs on the cloud chamber indicated whether one or both halves of the tray were struck.

As can be seen in Fig. 1, the solid angle of events accepted by the trays T and S, is slightly larger than the cone covered by the hodoscope counters. In this way, more efficient use is made of the available amount of absorber, even though some events accepted by the triggering system will not be covered fully by the hodoscope. Proper allowance for these losses will have to be made in estimating the energies of the showers.

III. ANALYSIS OF THE CLOUD-CHAMBER PHOTOGRAPHS

(1) Selection and Classification of Events

The arrangement described in the preceding section was operated at Echo Lake, Colorado (altitude, 3260 m) during the summer months of 1950, and at Syracuse, New York (altitude, 220 m) during the subsequent winter. A total of 402 cloud-chamber photographs were selected from these runs, of which about half were taken at Echo Lake. As no significant differences were observed between the characteristic features of the showers recorded in the two different runs, the following analysis will be based on all data without regard to altitude.

The selection of the cloud-chamber photographs was based on the recognition of a nucleonic event in the chamber. An event satisfying one or more of the following criteria was considered nuclear:

(a) *Penetrating showers;* these processes must show an ionizing primary and two or more secondaries capable of penetrating at least one lead plate without multiplication.

(b) *Stars;* i.e., events with one or more heavy prongs, providing the initiating particle is distinctly scattered.

(c) *Large showers* containing heavy prongs; high particle density may make it impossible to establish the penetrating character of secondaries, especially when a strong electronic component is present. The presence of star tracks is then taken as proof of the nucleonic character.

It is clear that most nuclear events taking place in the bottom plate of the chamber could not be identified on the basis of these criteria. In order to avoid a statistical bias from the inclusion of the few recognizable cases, all such events were discarded.

Besides genuine nucleonic events, the triggering system admitted also occasional knock-on showers, and, —very rarely—pure electronic showers of low density. The ratio of knock-on events to nucleonic showers proved useful in the determination of the energy of the primaries (Sec. V.2), but the analysis was confined to nuclear interactions.

One type of event frequently encountered was a low density air shower with an unusually high ratio of penetrating particles to electrons. It must be remembered that, in order to trigger the arrangement, one of the subtrays in T must register no hits. Besides, it often occurred that the extension tray showed either no hits, or hits in only one subgroup of counters. In many cases, several low energy nuclear interactions were observed in the chamber. In these events, the ratio of the number of electrons to N-particles was of the order one. Because of their frequency, it was concluded that these showers cannot be explained as the result of a large fluctuation in the particle ratio as it is found in showers not very far from the cascade maximum. They were interpreted as "tails" of old showers, in which the electronic cascade had been almost completely absorbed.

For the sake of clarity, a brief outline of the following analysis will be given here. The statistics of a number of features are unaffected by the bias which is introduced by the triggering arrangement. Thus, for instance, the interaction mean free path of the shower secondaries, or the relative number of protons, neutrons, and mesons (both charged and uncharged), may be determined directly from the photographs. On the other hand, in order to obtain the interaction mean free path of the primaries, or any statistics involving the multiplicity of the initial event, one has to take into account the different detection probabilities of the triggering arrangement. These probabilities have been computed in Appendices I and II, by considering (a) the development of the nuclear cascade in the plates below the primary event (transition effect), and (b) the geometry of the triggering arrangement as a function of the location of the primary event. The evaluation of (a) was, in turn, based on a careful study of the properties and composition of the shower secondaries, presented in the remaining paragraphs of this section.

(2) Range Spectrum of Relativistic Secondaries

In the following a secondary will be called relativistic, if it appears in at least one shelf with less than twice minimum ionization. In order to exclude electrons from this category we must further require that the particle be seen to penetrate at least one lead plate without cascade multiplication. The particles thus defined are known to dissipate energy both in gradual ionization losses and in more or less catastrophic collisions. A definite range may be assigned to the first process, a mean free path to the second.

For the slowest particles included in the above category, i.e., particles with twice minimum ionization in air, the ranges are about 80 g/cm² Pb in the case of protons, and between 15 and 20 g/cm² Pb for mesons. Thus, relativistic protons produced in the chamber will in general not be stopped in the chamber, while the

slowest relativistic mesons will be stopped in one or two lead plates. Also, some mesons which are emitted in a plate at relativistic speeds will emerge as heavy tracks and thus be missed in our statistics. The few relativistic protons that are stopped in the chamber, will in general be easily recognized.

A survey of stopped secondaries leads to the curves shown in Fig. 2. The data are divided into two groups according to the multiplicity of the primary event, ($N_s \leqslant 2$ and $N_s > 2$), and the fraction $\Phi(x)$ of particles absorbed in material of thickness x is plotted against absorber thickness.

Hodoscope data were included in this survey; this could be done without arbitrary normalization, as only the fraction of absorbed particles is recorded. However, the distinction between ionization losses and catastrophic collisions cannot be made as rigidly in the hodoscope as in the cloud chamber analysis. Secondary events with little penetration may have been missed if one particle continued without much scattering, or they may have been misinterpreted, if the secondary shower was entirely absorbed. Hence, the slopes of the absorption curves in Fig. 2 for thicknesses over 100 g/cm^2 must be considered a maximum rather than a correct measure of the ionization losses. But even though these absorption data are not quantitatively significant for large thicknesses, they clearly demonstrate the fact that the rather strong absorption observed in the cloud chamber holds only for one "component" of the secondary radiation.

The absorption curves of Fig. 2 can be expressed analytically by an expression of the form

$$\phi(x) = 1 - (ae^{-x/x_0} + be^{-x/X_0}), \qquad (1)$$

the parameters of which are: $x_0 = 45$ g/cm^2, $X_0 = 500$ g/cm^2, $(a+b) = 1$, and $a = 0.3$ for the lower multiplicity, $a = 0.4$ for the higher multiplicity. Clearly, only the first exponential is somewhat accurately defined by the curves, and with it the fraction a/b. But as X_0 is certainly large compared with the amount of absorber in the chamber, the following analysis will not depend on the accuracy of its determination.

(3) Composition of Showers

Positive identification of the shower secondaries can be carried out in the case of particles that are stopped or come close to the end of their range in the cloud chamber. Since this group comprises only a small fraction of all shower particles, and since the nature of particles which either leave the illuminated region, or traverse the chamber without appreciable energy loss, cannot be readily determined, an indirect method will be used to obtain, statistically, the composition of the showers.

The ratio of mesons to protons among the shower secondaries may be obtained from a comparison of the number of neutron-induced secondary nuclear interactions with the number of similar events initiated by

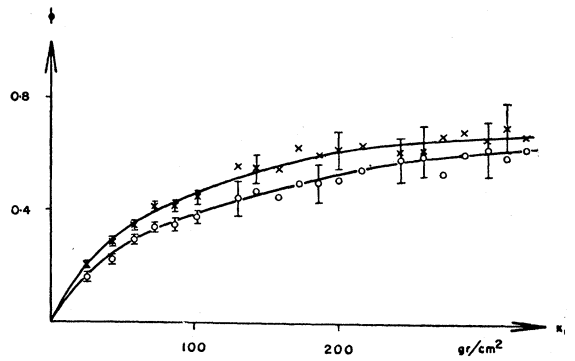

FIG. 2. Absorption of the secondaries: the fraction Φ of penetrating particles absorbed in x g/cm^2 Pb plotted against x for two multiplicity groups. Circles: $N_s \leqslant 2$; crosses: $N_s > 2$.

charged shower secondaries. The following assumptions are made in this analysis:

(a) The interaction mean free path is very nearly the same for π-mesons, protons, and neutrons.

(b) The numbers of energetic protons and neutrons in the showers are about equal.

Good evidence for the first point has been given by Tinlot and Gregory.[7] The second assumption appears justified on the basis of the neutron excess of the lead nucleus, the requirement of a charged primary, and the observed multiplicities of the nuclear events.

In selecting the secondary interactions for this analysis, care has to be taken to include only such events that leave no doubt as to whether they were initiated by an ionizing or neutral particle. This method should introduce no bias on the observed ratio of neutral-induced to charge-induced events, since these two types of events showed no observable differences, and should therefore be detected with equal probabilities. On the other hand, this selection will not be representative of either the total frequency of secondary nucleonic events for different primary energies, or the location of the secondary showers. In large primary events, for example, and especially near their origin, the identification and classification of secondary events becomes much more difficult.

Out of a total of 108 secondary events, 34 were found to be neutron-initiated. If again the primary events are grouped according to the multiplicity of their penetrating secondaries, one obtains for the group of lower multiplicities ($N_s \leqslant 2$) 21 "neutrals" out of a total of 58 events, and for the group of higher multiplicities ($N_s > 2$) 13 "neutrals" out of 50 events. With the assumptions made above, this gives for the ratio of fast π-mesons to protons emitted in these collisions a value of 0.76 for the first group of multiplicities, and 1.85 for the second, with an average of 1.2 ± 0.3 for all showers observed in this experiment. It should be pointed out that the probable error given above takes into account the fact that a number of secondaries can be positively identified as either protons or mesons,

and is therefore somewhat smaller than the statistical fluctuation. In the subsequent analysis the ratio $r_p=N_p/N_s$ of penetrating protons to ionizing shower secondaries will be introduced; for $N_s\leqslant 2$ this is 0.56, and for $N_s>2$ it becomes 0.35.

It may be noticed that the ratio N_π/N_p is larger in both multiplicity groups than the empirical ratios a/b derived in the preceding paragraph. It follows that the less penetrating "component" in Eq. (1), with its average range of 45 g/cm^2 is not representative of the entire meson spectrum, but only of its low energy portion which makes up about one-half of the total meson component.

(4) The Electron Component

"Mixed showers," i.e., nuclear events accompanied by an electronic cascade, were observed in 191 cases out of 327 for which certain identification of the presence (or absence) of an electronic shower was deemed possible. In many of these events, however, the picture did not permit a clear determination of the number of electron cascades originating in a collision. Consequently, the values given here for the number of mesons emitted per interaction and the ratio of π^0 mesons to charged π-mesons should be considered lower limits.

TABLE I. Observed size distribution of electron showers for primary interactions of different multiplicity.

Number of electrons		3	4–6	7–9	10–12	13–15	15
Number of showers observed	$N_s\leqslant 2$	5	15	21	22	13	9
	$N_s>2$	2	5	10	19	31	39

If one assumes now that in all observed mixed showers a single neutral meson was responsible for the electronic component, one obtains from the 85 mixed events among 207 showers with two or less penetrating secondaries, a value of 0.41 neutral meson per shower, or, using the results from the preceding paragraph, 0.55 ± 0.15 neutral meson per charged meson. Likewise one finds among the showers with more than two penetrating secondaries, 106 mixed events out of a total of 130 showers, which yields 0.82 neutral meson per shower, or 0.36 ± 0.1 neutral meson per charged meson.

The error in these values due to the initial assumption of single neutral mesons is likely to be negligible for the low multiplicity group of showers, but may well be substantial in the case of high multiplicities. In the subsequent calculations a ratio of 0.5 neutral meson per charged meson was used. This value agrees well with the older measurements of the Bristol group[16] obtained in nuclear emulsions, though not so well with their later value[17] of 1.0 ± 0.3. Using a cloud chamber, Salvini and Kim[18] have recently found a ratio of 0.37 ± 0.08.

In an attempt to estimate the energy of the π^0 mesons, the total number of electrons at maximum development of the common cascade was determined, wherever it was impossible to resolve the electron component into individual cascades. This procedure gives the correct answer if all of the decay energy of the neutral meson goes into one of the photons, and a very nearly correct answer if the energy is equally divided, because of the almost linear increase of the number of electrons at the cascade maximum with the energy of the initiating photon. It is also a good approximation for most of the intermediate region because of the slow variation of the particle number in the neighborhood of the cascade maximum. The frequencies of the electron showers of various sizes at maximum development were thus determined, either by adding the numbers of particles at the respective maxima, where the showers could be separated, or by taking the number of particles at the apparent maximum of the combined cascade in the other case. The results are listed in Table I.

The average initial energy of the cascades can now be calculated from the tables of Bhabha and Chakrabarty.[19] The values thus obtained are about 600 Mev and 850 Mev for the lower and higher multiplicity groups, respectively. The first value agrees well with the data of Salvini and Kim,[18] the second is possibly too high, since one would expect an appreciable fraction of these events to be due to the decay of more than one neutral meson. On the other hand, a higher average energy per neutral meson seems reasonable in view of the higher average primary energy which one can infer from the higher multiplicities.

(5) Multiplication of Shower Secondaries

The interaction mean free path of penetrating shower secondaries has been measured in numerous experiments, both with cloud chambers[2,6,7,20,21] and nuclear emulsions.[17,22] Some of the results differ rather widely. It has been generally conceded that the values obtained with cloud chambers are too high, unless thin plates are used and great care is taken not to miss small interactions of low penetration. The present experiment with its $\frac{1}{2}$-inch plates is thus not well suited for a redetermination of the interaction mean free path. However, an evaluation of this quantity is required for the determination of the transition effect of penetrating

[16] Carlson, Hooper, and King, Phil. Mag. **41**, 413 (1950).
[17] Camerini, Davies, Fowler, Franzinetti, Muirhead, Lock, Perkins, and Yekutieli, Phil. Mag. **42**, 1241 (1951).
[18] G. Salvini and Y. Kim, Phys. Rev. **85**, 921 (1952). We are indebted to these authors for communicating their results before publication.
[19] H. J. Bhabha and S. K. Chakrabarty, Phys. Rev. **74**, 1352 (1948).
[20] Lovati, Mura, Salvini, and Tagliaferri, Nuovo cimento **7**, 145 (1950).
[21] Butler, Rosser, and Barker, Proc. Phys. Soc. (London) **A63**, 145 (1950).
[22] Camerini, Fowler, Lock, and Muirhead, Phil. Mag. **40**, 1073 (1950).

particles in the chamber and the resulting bias imposed on the triggering system (Appendix II). Thus, while the mean free path as derived from the "observable" secondary showers represents only an upper limit, it is this quantity which actually determines the necessary corrections for the transition effect, since the small interactions that are readily absorbed in one plate will produce no counts at the S-tray.

Events were considered "observable" if either one relativistic secondary accompanied by at least one heavy track was seen to emerge from the lead plate, or at least two relativistic secondaries appeared below the plate, or if the incident relativistic particle is scattered by more than 15°.

A total of 122 secondary interactions satisfying the above conditions were found. This number includes the 108 events discussed in Sec. III.3, as well as those events that were left out in the previous statistics because of ambiguity in the nature of the initiating particle. Since we can compare the number of interactions only with the number of traversals of lead plates of charged shower particles, the number of "charge-initiated" interactions among the 122 will have to be determined. We may assume for this purpose that the 14 ambiguous events contain the same fraction of "neutrals" as the other 108. The total number of secondary events initiated by charged particles is then 84. Comparing this with a total of 1246 traversals of $\frac{1}{2}$-inch lead plates under an average zenith angle of 30°, one obtains an interaction mean free path for "observable" events of $\Lambda_s = 250 \pm 30$ g/cm² Pb.

The average multiplicity of penetrating charged particles in the secondary showers is rather low: about 1.5. Within the limited statistical accuracy attainable, no difference could be observed between the showers secondary to large or small primary interactions.

IV. ANALYSIS OF THE HODOSCOPE DATA

(1) The Integral Path Length

The procedure of obtaining an estimate on the energy of the primary from the hodoscope records will involve two major steps: (a) that of estimating from the distribution of counters struck the integrated absorber thickness traversed by all the penetrating charged particles of the nuclear cascade in the hodoscope, and (b) the assignment of a primary energy to each of these "integral path lengths."

The first step involves the application of certain statistical and individual corrections to the hodoscope pictures. The statistical corrections must take into account "losses" due to particles missing counters in traversing a tray, or counters being struck by more than one particle; they must also take into account the "gains" that are caused by the discharge of more than one counter in a tray with the passage of a single inclined particle, or a particle accompanied by a low energy knock-on. The individual corrections must take into account the losses due to the fact that, in general, only a fraction of the cascade lies in the solid angle covered by the hodoscope.

In order to estimate the statistical corrections for single particle traversals, hodoscope pictures were taken in a test run during which the arrangement was triggered by single penetrating particles. The efficiency of the hodoscope trays was determined from the number of "blanks" in well-defined "tracks" which could be followed through at least three trays. The same events were examined for simultaneous discharges of two or three neighboring counters of the same tray which were interpreted as being due to knock-ons and track inclination. Events that showed the discharge of several not neighboring counters in one tray, or the discharge of several counters in two or more successive trays, were not included in this survey, but interpreted as nuclear interactions. The result of this test run was a value of about 95 percent for the efficiency of all five trays, a "double discharge" rate for single penetrating particles of 6 percent, and a "triple discharge" rate of 1 percent per counter struck. If each lighted neon bulb is counted as a "traversal," the correction factor to be applied is, therefore, 1.01, which is practically insignificant.

The correction for the discharge of one counter by more than one particle is both more serious and more difficult to evaluate. For a rigorous treatment, one would have to know the lateral density distribution of the shower particles. For a random distribution the exact solution has recently been obtained by Schrödinger.[23] Although the shower particles are certainly not distributed at random over the counter area, the following considerations indicate that the error made in applying Schrödinger's formula is probably small: Unless the shower is produced very close to the tray, a small number of counters struck means a low particle density; hence, the correction will be small regardless to the distribution. A high particle density, on the other hand, will usually represent cases in which several interactions contributed, so that the distribution will approach a random character. It is, therefore, believed that the corrections based on the assumption of a random distribution will be satisfactory.

In making the individual corrections, the fraction of the cascade covered by the hodoscope trays was estimated for each shower. Only those events were included in the statistics, for which this fraction exceeds one-half. This correction, then, merely consists of dividing the path length observed by the fraction determined for that shower.

In reading the path lengths from the hodoscope picture it is assumed that the particles will, on the average, stop halfway between the last counter struck and the next tray. Thus a path length of 6-in. Pb $+\frac{1}{4}$-in. Fe is assigned to particles entering the hodoscope

[23] E. Schrödinger, Proc. Phys. Soc. (London) **A64**, 1040 (1951)

TABLE II. Observed frequency of showers with integral path length exceeding L g/cm² (both individual and statistical corrections are applied).

L (g/cm²)	380	760	1140	1530	1910	2290	2670	3050
Number of showers	363	259	184	149	111	87	60	47

from the chamber and reaching the first tray, and a length of 4-in. Pb+¼-in. Fe for each further tray traversed.

The resulting distribution in integral path lengths is shown in Table II, which lists the number of showers with a path length exceeding L, after both statistical and individual corrections have been applied.

In parts of the survey, hodoscope records were also included for which the corresponding cloud-chamber picture was of too poor quality for satisfactory analysis, or where no cloud-chamber pictures had been taken. It was required then that the location and direction of the shower in the hodoscope gave reasonable assurance that not just the fringes of a shower had been registered. A total of 412 hodoscope records were analyzed in this way.

(2) Secondary Interactions

Qualitatively, the existence of cascade-type multiplication in nucleonic showers is very clearly demonstrated by the hodoscope records of this experiment. If, for instance, the average number of counters struck per tray is plotted against absorber thickness (Fig. 3), one obtains unmistakable evidence for a positive transition effect. A quantitative analysis, however, if it were to be carried out rigorously, would encounter enormous difficulties, which are primarily due to the thick absorbers used here.

It was therefore decided to study only two special features from which limited evidence on the interaction mean free path of the shower secondaries may be derived.

The number of incident particles is best known for the top layer of absorber in the hodoscope, from the corresponding cloud-chamber photograph. Since this number is in general low, most secondary interactions taking place in the top layer can be detected and counted on the basis of the record of the first tray of counters in the hodoscope. It is clear that such a count can furnish us only with a lower limit for the total number of interactions, since events of low penetration are likely to be missed. A mean free path obtained from this analysis will thus be representative of only high energy events. In making the calculations, one has to add to the number of relativistic tracks that are seen to leave the chamber in the proper direction, the corresponding number of fast neutrons, in order to obtain the total flux of interacting particles incident on the hodoscope. This number can be evaluated from the results of the cloud-chamber analysis discussed in Secs. III.2 and III.3.

Corrected in this way, the 645 charged particles incident on the hodoscope in 382 analyzed showers, correspond to a total flux of 1050 interacting particles. A count of one nuclear interaction was registered for each of the following observed events: the discharge of two counters separated by a gap of at least one 1-inch counter, or the discharge of at least three counters, in a region of the hodoscope where not more than one particle was incident, or an increase of the number of counters struck over the number of particles incident of at least two. Thus, 324 such interactions were found, which leads to a maximum mean free path of 345±40 g/cm² for collisions with considerable energy transfer.

A second group of nuclear interactions could be identified wherever it was possible to follow individual particles through at least three trays. Large angle scatterings, exceeding 20°, were selected. In a large fraction of these events no other "tracks" were seen to emerge, indicating that one is dealing here with rather low energy interactions which are about complementary to those described above. In this group 117 particles showed 48 such interactions in 383 traversals. From this one calculates a mean free path of about 960 g/cm² for these collisions. If these two types of interactions covered the entire range of possible interactions without overlapping, one would derive from the above a total mean free path of about 250 g/cm².

(3) The Primary Energies

While the integral path lengths recorded in the hodoscope certainly convey qualitatively a good picture of the primary energies, the procedure of translating them into quantitative data is neither simple nor unambiguous. A good part of the arbitrariness can be eliminated by using the information gained in the cloud-chamber analysis as a guide in the interpretation of the data. Finally, a comparison of the shape of the energy spectrum and the intensity of the proton component deduced in this analysis with the results of earlier

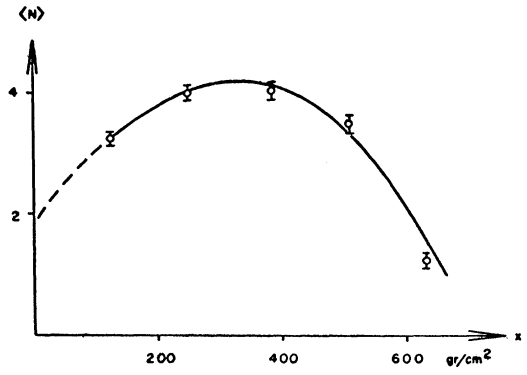

FIG. 3. Transition effect in the hodoscope pile: Average number $\langle N \rangle$ of counters struck, plotted against the absorber thickness x. The errors shown include only statistical deviations.

experiments will serve as a check on the assignment of energies to the observed integral path lengths. The agreement found in both cases is good, which gives one confidence in the soundness of the method.

As a first step, it will be assumed that the recorded paths are all due to the passage of penetrating particles of the nuclear cascade. This will certainly be very nearly true since, in view of the thick absorbers, most events will occur sufficiently far away from the nearest tray to prevent any slow particle and most electronic cascades from reaching the counters. The first problem is, then, to estimate correctly the average ionization loss of the penetrating shower particles. For the mesons, a value close to the minimum ionization will certainly be adequate; while for the protons this value would represent a serious underestimate of the energy dissipation, since in a cascade the number of traversals of protons of a few hundred Mev—"gray tracks"—, in general, exceeds that of the faster particles. In some of the less dense showers an average range of cascade particles, between two and three traversals, could be observed in the hodoscope. Since, for the larger events, the fast energy degradation typical for collisions in lead will soon establish similar conditions, the mean ionization corresponding to that range (1.8 Mev/g/cm)[2] may be taken as a fair average for all cascade protons. Similarly, the ratio of mesons to protons will soon be reduced to an average characteristic for low energy events, regardless of the energy of the particles incident on the hodoscope. For such a mixture, the mean ionization will be in the neighborhood of 1.6 Mev/g/cm^2. Thus, for an integral path length L, the total energy dissipation of the penetrating particles, which is the result of ionization losses, may be taken as $L\times 1.6$ Mev. While this method may perhaps involve an error of as much as 10 percent in the absolute value of the energies, it will not introduce a significant bias between the groups of different primary energies.

There are, of course, a number of items that have yet to be taken into account in the energy determinations. These are:

(a) the energy in relativistic particles which do not reach the hodoscope (shower particles of low penetration and electronic component);
(b) binding energies;
(c) energies of neutral particles;
(d) energies of heavily ionizing "star" particles.

The corrections (a) through (d) turn out to be very appreciable. The following is a brief summary of the methods applied:

(a) The energy of the electron cascades initiated in the cloud chamber was determined from the total number of electrons at the maxima (or maximum), as in Sec. III.4. The correction for the energy transfer to the electron component initiated in collisions in the hodoscope pile will be outlined in (c). As to the low energy shower particles, only the charged mesons have to be considered. The ranges were either observed directly in the cloud chamber, wherever this was possible, or the range distribution of Sec. III.2 was used.

(b) A binding energy of 8 Mev per nucleon, and of 140 Mev per meson was assumed. For each primary interaction, the meson-to-proton ratio derived empirically for showers of that multiplicity was taken as a basis for computing the "average binding energy" supplied. Likewise, all subsequent interactions in the chamber and the hodoscope, were classified as to their multiplicities, and the corresponding binding energy corrections were determined. In complex events for which not even mean multiplicities could be established, an estimate was made from the observed penetration of the cascade.

(c) The number of neutrons is again assumed to be equal to that of the protons, and was determined from the observed multiplicities and the shower composition found in Sec. III.3. According to Sec. III.4, the number of neutral mesons is about one-half of that of the charged mesons. It was estimated from their energy distribution that about $\frac{2}{3}$ of them would not be registered in the hodoscope. With the help of the multiplicities derived in (b) and of the mean energies of Sec. III.4, the correction can now be worked out.

(d) According to the results of the Bristol group,[17] the number of heavy prongs varies rather slowly with the number of shower particles, or with the kinetic energy of the primary particle. Besides, their contribution to the energy dissipation amounts to less than 10 percent for high primary energies, while their relative importance is, of course, much greater for small showers. The correction applied here must also include a small fraction of the "gray tracks." An average of 150 Mev per interaction was considered reasonable for the total effect, and the total number of interactions was estimated by dividing the integral path length by the most likely value for the interaction mean free path for low energy collisions (270 g/cm^2). At any rate, the error in the primary energy that results from a wrong estimate of this correction is rather small.

Following this procedure, the primary energy could be obtained for each event recorded in the cloud chamber. Fluctuations in the fraction of the primary energy intercepted by the hodoscope may make some of the individual values badly inaccurate, especially when the hodoscope covered not much more than one-half of the shower cone. However, as each measurement also includes a considerable number of cascade interactions, the fluctuations will be smoothed out by the secondary and subsequent collisions, and the results for the primary energies will be, at least statistically, significant.

V. RESULTS AND DISCUSSION

(1) The Primary Mean Free Path

The distribution of primary events over the upper seven lead plates of the cloud chamber is shown in

TABLE III. Number of the nuclear interactions recorded in the first seven lead plates, divided into "multiplicity groups" according to the number N_s of penetrating secondaries.

Plate		1	2	3	4	5	6	7
Number of showers recorded	$N_s \leqslant 2$	37	33	30	31	29	30	27
	$N_s = 3$	16	13	14	10	11	10	10
	$N_s \geqslant 4$	10	9	9	7	8	5	6

Table III, which is obtained directly from the photographs. The events are here grouped according to the multiplicities of penetrating secondaries. As pointed out before, these rates cannot be used directly for an evaluation of the interaction mean free path of the primaries because of the varying bias introduced by the triggering system. The detection probabilities were computed in Appendices I and II, and are tabulated in Table IV. One can now determine the unbiased shower rates, and from these the mean free path of the primaries. The events may also be regrouped now, using their energy rather than their multiplicity for the classification. Thus, the mean free path may be obtained as a function of the primary energy.

One needs to know for this the total number of charged N-particles which have traversed the chamber during its operating time. If this number is called N_0, then the number I_x of primary interactions occurring in the first x cm of absorber is given by

$$I_x = N_0(1-e^{-x/\Lambda}). \tag{2}$$

Applying Eq. (2) to two thicknesses X and $\xi = X/2$ and eliminating Λ between the two equations, gives

$$N_0 = (I_\xi)^2/(2I_\xi - I_X). \tag{3}$$

The fractions N_x/N_0 of particles traversing a thickness x without interaction are shown in Fig. 4, plotted logarithmically against x, for three energy groups: $E_p \leqslant 2$ Bev, 2 Bev $< E_p < 4$ Bev, and $E_p \geqslant 4$ Bev. The collision mean free paths computed for these three

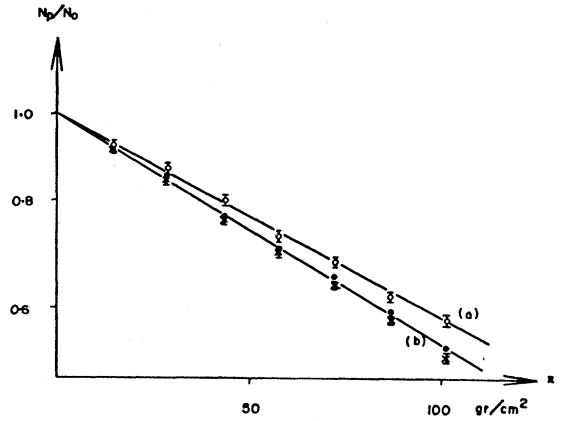

FIG. 4. Fraction N_x/N_0 of charged N-particles that penetrate x g/cm² Pb without interaction. Empty circles: $E_p \leqslant 2$ Bev; full circles: 2 Bev $< E_p < 4$ Bev; crosses: $E_p \geqslant 4$ Bev. Calculated curves (a): interaction mean free path $\Lambda = 190$ g/cm²; (b) $\Lambda = 160$ g/cm².

energy ranges are, respectively: 190±15 g/cm², 168±18 g/cm², and 152±15 g/cm². The difference between the two extreme values appears significant. For the middle group no certain conclusion can be reached. If it is included in the group of highest energies, the mean free path for N-particles with energies exceeding 2 Bev is found to be 158±12 g/cm², in good agreement with the "geometrical" value of 165 g/cm², and with numerous earlier observations on showers of high multiplicity and penetration. However, a remarkable discrepancy appears to exist between these results and those of most of the counter experiments,[8–11] where usually a considerable increase of Λ with decreasing multiplicity and penetration, interpreted as decreasing energy, of the shower was observed. The present results would demand an assignment of average primary energies below 1 Bev for these penetrating showers, and this appears definitely too low. The explanation may lie in the inefficiency of most counter experiments to detect small interactions of low penetration occurring in the top absorbers. As it will be shown in Sec. V.3, such collisions are by no means very rare for primary energies of a few Bev.

A cloud-chamber arrangement of the kind applied in this experiment will record these interactions as "stars," but it will miss them if the primary particle should undergo a charge exchange in the collision. It is tempting to interpret the difference between the mean free path of the lowest energy group and the "geometrical" value as the result of this failure of the triggering system to include charge-exchange interactions of low multiplicity. It will be seen from the data of Sec. V.3 that this would require a probability of about (0.25 ±0.15) for charge exchange in a collision with only one penetrating secondary.

TABLE IV. Triggering probabilities $W(\rho, N)$ for showers of various multiplicity groups initiated in the lead plates.

Plate		1	2	3	4	5	6	7
$W(\rho, N)$	$N_s \leqslant 2$	0.212	0.196	0.184	0.190	0.210	0.242	0.224
	$N_s = 3$	0.448	0.430	0.408	0.390	0.422	0.450	0.444
	$N_s \geqslant 4$	0.614	0.590	0.576	0.570	0.602	0.640	0.604

(2) The Primary Energy Spectrum

With the interaction mean free paths, the detection probabilities, and the observed shower frequencies, it is now possible to determine the relative intensities of the shower primaries for different portions of their energy spectrum. The differential primary spectrum thus obtained is reproduced in the step curve of Fig. 5.

The results render support to the procedures employed in Sec. IV.3 to determine the absolute values of the energies. The energy distribution obtained is in good agreement with the spectrum observed by Mylroi and Wilson[24] who report a differential momentum spec-

[24] M. G. Mylroi and J. G. Wilson, Proc. Phys. Soc. (London) **A64**, 404 (1951).

trum of the form $S(p) \propto p^{-2.8}$. Their sea-level data agree with the data taken at 30,000 feet by Adams *et al.*,[25] showing that the proton spectrum no longer varies greatly with atmospheric depth, once its low energy part is "filled in." The absence of noticeable differences in the events observed with the present equipment at Syracuse and at Echo Lake, confirms that result. The spectrum of Mylroi and Wilson is shown in the smooth curve in Fig. 5.

The intensity of the charged N-component relative to that of the total hard component can be estimated by comparing the rates of genuine nucleonic events (after applying the corrections for the detection probabilities) with the rate of knock-on events showing the passage of a single penetrating particle. The probability that a penetrating particle produce a knock-on that is detectable in the S-tray, was determined by taking the telescope rate of single penetrating particles traversing the chamber, and of single penetrating particles that trigger two neighboring counters separated by lead strips of $\frac{3}{4}$-in. thickness and $1\frac{1}{2}$-in. height. With the geometry of this experiment, the knock-on rate was only 0.35 percent of the telescope rate. At Echo Lake,

TABLE V. Average multiplicities $\langle N_s \rangle$ of all penetrating secondaries, average multiplicities $\langle N_\pi \rangle$ of charged mesons, and average energies ϵ_s per charged secondary, as a function of the primary energy E_p.

E_p(Bev)	1–2	2–4	4–6	>6
N_s	1.6 ±0.1	2.2±0.14	3.5±0.19	4.9±0.27
N_π	0.48±0.25	1.5±0.65	1.2±0.60	3.3±0.65
ϵ_s (Bev)	0.50	0.70	0.81	0.97

about two out of every five cloud-chamber pictures showed nongenuine triggers due to single penetrating particles with knock-on accompaniment. From this, one obtains a value of about 2.5 percent for the ratio of charged N-particles above 1 Bev to the number of all hard particles. The data of Tinlot and Gregory[7] taken at the same altitude give a ratio of about 2 percent for the same energy range.

At Syracuse the "knock-ons" exceeded the genuine events by a factor 7:1. The corresponding ratio of N-component to total hard component is 0.28 percent, which again agrees very well with the 0.25 percent found near sea level by Mylroi and Wilson.[24]

The satisfactory agreement of both the spectral distribution and the absolute intensities obtained in this experiment with the results of earlier measurements of other authors proves that the energy values derived in Sec. IV.3 are more than qualitatively correct.

(3) The Shower Secondaries

The energy determinations are finally used to investigate the dependence of shower multiplicity and shower composition on the energy of the primary particle. All recorded events were therefore re-grouped according to their energies. The resulting statistics are shown in Table V.

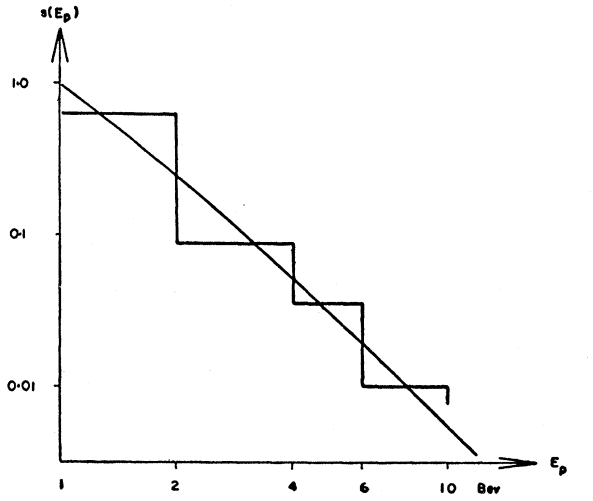

FIG. 5. Differential energy spectrum of the shower primaries. The smooth curve represents the results of Mylroi and Wilson, the step curve the data obtained in this experiment.

The first row in Table V gives the average multiplicity $\langle N_s \rangle$ of all charged penetrating secondaries after correcting for the bias of the arrangement in the manner described in the appendices. The second row shows the average number $\langle N_\pi \rangle$ of π-mesons among the secondaries. This quantity was computed as in Sec. III.3 from the survey of secondary interactions, and checked against direct evidence from the pictures. The average energies $\langle \epsilon_s \rangle$ given in the third row were obtained by dividing the primary energy by $\langle N_s \rangle$ after subtracting the binding energies, the energy carried by the electron component, and the energy of particles of more than twice minimum ionization, including the "star" energy of about 200 Mev.

Similarly, the relative frequency of events of different multiplicities has been plotted for the various energy ranges in Fig. 6. In addition to the penetrating charged secondaries, neutral mesons are included in this summary, either in their accurate number, where the electron cascades could be resolved, or as single particles. The diagrams show, therefore, not fluctuations in the ratio of charged and neutral mesons emitted, but a genuine spread in the emission of secondaries.

It is of interest to note that of all the primaries of more than 4 Bev energy, only six initiated in the chamber are small showers with not more than one penetrating particle. In two cases an electron cascade was present, while three collisions showed only heavily ionizing secondaries emerging with the penetrating particle. Only one case showed large angle scattering without observable secondaries. This latter event, and two of the others, were followed by a large shower in a lower plate.

[25] Adams, Anderson, Lloyd, Rau, and Saxena, Revs. Modern Phys. **20**, 334 (1948).

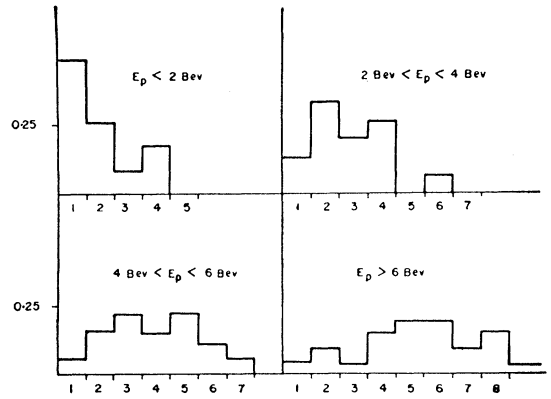

FIG. 6. Multiplicity distribution of shower secondaries (including neutral mesons) for various primary energy ranges between 1 Bev and 10 Bev.

The distribution of energy transfers to the neutral meson component is represented in Fig. 7. The energies were determined as in Sec. III.4 from the observed total number of electrons at the maximum of the common cascade, or, where a resolution into individual cascades was possible, by adding the numbers of electrons at the respective maxima. As at least some of the cascades are certainly initiated by more than one meson, the curves of Fig. 7 should not be interpreted as the energy spectrum of the π^0 mesons. That spectrum is evidently steeper than the distributions shown.

(4) Conclusions

In a recent summary of the extensive work on meson production in nuclear collisions carried out by the Bristol group, Camerini *et al.*,[26] compare the results obtained from observing events in photographic emulsions with the various theories of fast collisions.[12,14,15] They find that both the multiple and the plural theory can account for the experimental facts, if secondary nucleon-nucleon and meson-nucleon collisions are also considered.

In spite of the indirectness in the derivation of some of the present results, similar and, in some respects, additional evidence can be deduced from these data. The advantage of a study of interactions in lead is the homogeneity of the target material and the larger dimensions of the interacting nucleus, which makes the collisions more sensitive to second-generation effects.

It has already been shown in the Bristol analysis[26] that the average multiplicities prove a poor test for the theories, at least for primary energies below 10 Bev. In every case parameters can be found that will make the theory agree with experimental results. In particular, the plural theory yields a quite satisfactory agreement if the fractional kinetic energy loss σ of the primary, and its distribution between recoil nucleon and meson, have the values suggested by Heitler ($\sigma=\frac{1}{4}$, equally divided). Messel's[27] constants can also be made to agree, if meson production by recoil nucleons is included.

The ratio of π-mesons to nucleons among the shower secondaries found for the showers in lead is similar to that of the showers initiated in nuclear emulsions. Its large value has been explained by Heitler and Therreaux[28] on the basis of the plural theory as the result of "many-body collisions" of the primary and the successive recoil nucleons with the same nucleon "at rest." The similarity of the results in the two widely different materials would then suggest that this mechanism remain effective for all the meson-producing collisions, and, hence, that in general the energy degradation in the lighter nuclei suffices to carry the primary below the cut-off energy for multiplication. The larger spread of the showers in lead is then mainly due to subsequent elastic collisions.

The distribution of multiplicities shown in Fig. 6 reflects variations in the degree of inelasticity, or in the energy of the mesons emitted. Again both theories can explain the wide spread observed both in this experiment and in the photographic emulsions. The plural theory would certainly demand this result if a transfer law of the kind suggested by Heitler and Janossy[14] is assumed, providing again that the energy degradation is fast (large σ). This latter condition is also suggested by the similarity of the results obtained in emulsions and in the cloud chamber, at least up to primary energies of 10 Bev.

The comparatively slow variation of the average energies of the secondaries with the primary energy, finally, provides another argument for either the multiple theory, or the plural theory with a σ larger than Heitler's value. It is unfortunate that a separation of the two components among the shower secondaries was not possible, so that this argument cannot be followed in all possible details. The large fraction of low energy mesons, demonstrated by the absorption curves (Sec. III.2) suggests again a high probability for small energy transfers, or a large contribution due to recoil nucleons if interpreted on the basis of the plural theory.

Thus, while not enough material is as yet available to definitely prove or disprove any specific theory, more stringent conditions can be imposed, especially on the plural theory: On the one hand, the fractional transfer of kinetic energy must fluctuate widely in individual collisions, and its mean value must be larger than that suggested by Heitler. On the other hand, interactions of the recoil nucleons must certainly be considered. Whether or not the results will be compatible with the experimental data if meson collisions are also included,—and the more recent observations leave no doubt that the high degree of transparency of the nucleus to mesons, originally assumed by Heitler

[26] Camerini, Davies, Franzinetti, Lock, Perkins, and Yekutieli, Phil. Mag. **42**, 1261 (1951).

[27] H. Messel, Proc. Phys. Soc. (London) **A64**, 726 (1951).

[28] W. Heitler and M. Therreaux, quoted in reference 26.

and Janossy, is not justified,—cannot be decided on the basis of this experiment. More data, preferably obtained in a more direct way, will be required.

The work described here was supported in part by the Atomic Energy Commission. Operation at Echo Lake, Colorado, was made possible by the facilities of the Inter-University High Altitude Laboratory, and through the friendly cooperation of its officials, in particular Professor Byron Cohn and Professor Mario Iona, Jr., of the University of Denver. Mr. J. J. Kraushaar, Mr. E. Plofker, and Mr. H. L. Kasnitz have assisted at various phases of preparation and operation of the experiment.

APPENDIX I. THE GEOMETRICAL BIAS OF THE SELECTION SYSTEM

(1) The Triggering Probability

The statistical corrections that are to be applied to the observed shower rates to give the true frequencies of the various events, will be computed by treating separately two aspects of the problem:

(a) the "geometrical bias" of the system of counters that define the masterpulse;

(b) the "transition effect," i.e., the change in the number of penetrating particles that reach the S-tray, owing to absorption and multiplication.

The following simplified picture of a typical nuclear event will illustrate the methods employed: An ionizing primary has struck one counter in traversing the T-tray and produces in one of the lead plates an interaction in which N_s penetrating charged secondaries are emitted into a cone of given angular spread. The secondaries are assumed to be distributed in a random manner over the solid angle of that cone and will, in traversing the subsequent plates, experience secondary interactions with a mean free path as determined in Sec. III.5 and range absorption as a result of ionization losses according to Sec. III.2. The cone occupied by the resulting "cascade" will not be very much different from the cone of secondaries of the primary interaction, and will contain at the level of the S-tray, N shower particles randomly distributed over an elliptical area which is the intersection of the cone and a plane through the S-tray. Thus, each of the N particles will have the same probability ρ of striking a counter in S, depending on the size of the ellipse and its position relative to the S-tray. The probability of producing a masterpulse (i.e., of producing at least one count in each of the two subtrays of S), can now be expressed as a function of ρ and N. Here ρ will depend on the location of the primary event, its zenith angle, and the angular spread of the cone of secondaries, while N must be determined from the "transition effect" as a function of the initial multiplicity N_s and the amount of absorber traversed by the cascade. It may be noted that the bias imposed by the T-tray and the effect of the limited counter efficiency can be neglected as long as one does not attempt to determine the absolute intensities.

The probability that out of the N particles which reach the level of the S-tray, n will strike a counter in S, may be written as

$$P(\rho, n, N)=\binom{N}{n}\rho^n(1-\rho)^{N-n}, \tag{4}$$

and the probability $p(n)$ of all n particles hitting the same subtray in S is

$$p(n)=(1/2)^{n-1}.$$

Thus, if $w(\rho, n, N)$ is the probability that n out of N particles will produce a masterpulse, one finds

$$w(\rho, n, N)=P(\rho, n, N)[1-(1/2)^{n-1}]. \tag{5}$$

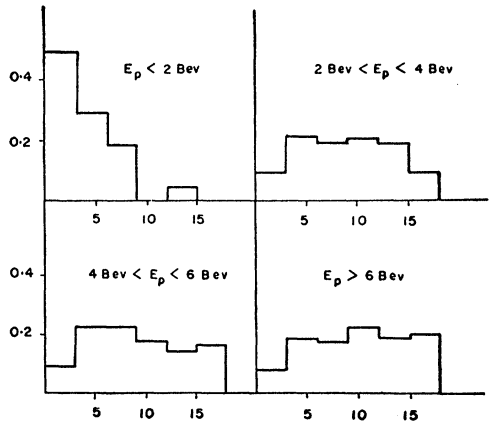

FIG. 7. Multiplicity distribution of electron showers for various primary energy ranges between 1 Bev and 10 Bev.

Since a minimum of two particles is required to trigger the S-tray the triggering probability for an N-particle shower is obtained by summing the expression (5) from $n=2$ to $n=N$:

$$W(\rho, N)=\sum_{n=2}^{N} w(\rho, n, N)=\sum_{n=2}^{N}\binom{N}{n}\rho^n(1-\rho)^{N-n}[1-(1/2)^{n-1}]. \tag{6}$$

The summation in Eq. (6) can be performed and gives the more convenient expression

$$W(\rho, N)=1+(1-\rho)^N-2(1-\tfrac{1}{2}\rho)^N. \tag{7}$$

(2) Zenith Angle and Angular Spread

The zenith angle of the shower primaries has a twofold effect: by increasing the amount of absorber traversed per lead plate it will produce a shift in the statistics on the penetration of the primaries, and it will be one of the factors determining the probability ρ with which the shower particles strike a counter in S. The first is an individual correction to be applied to each shower in determining the penetration of its primary. Thus, assuming that the primary interactions were on the average produced halfway through the plate in which they were observed, the actual penetration of the primary was computed from the number of traversals and the zenith angle observed for that event. This causes a slight change in the data listed in Table III, shifting some events to thicknesses larger than that indicated by merely compiling the plate thicknesses, and reducing the total number of showers produced within the 100.8 g/cm² (corresponding to 7 plates) by a few counts.

The effect of the zenith angle on the probability ρ is taken into account by assuming all shower primaries to enter the arrangement with an average zenith angle $\bar{\phi}$. This can be done because of the rather steep distribution of the particles and the additional bias which the system imposes in favor of vertically incident primaries. This assures the inclusion of primaries of a comparatively narrow cone only, over which a variation of the primary energy with the zenith angle is certainly negligible.

The angular spread of the showers will also affect the probability ρ. As mentioned above, this angle may be set equal to the opening of the cone of the nuclear cascade in the chamber, because the secondary events will generally occur close to the S-tray and will be of relatively low multiplicity. Again, the average of all observed angular spreads was used in the correction.

The average zenith angle observed was $\bar{\phi}=15°$, and thus only slightly less than the value computed for a $\cos^6\phi$ distribution ($\bar{\phi}=17.5°$), showing that the bias of the arrangement does not change the distribution greatly. The average angular spread of the penetrating secondaries, obtained directly from the observed cones, is $\bar{\theta}=23°$. No statistically significant difference between smaller and larger showers was found.

(3) Determination of the Probability ϱ

The slight variations of the triggering probability with the horizontal position of the shower origin were neglected in this analysis, and the computations were made for events located on the vertical chamber axis. Thus, for events initiated at a height h above the S-tray, the intersection of the shower axis with the plane S will lie on a circle of radius $R=h\tan\bar{\Phi}$, if all shower primaries are assumed to have the same zenith angle $\bar{\Phi}$. If now all angular spreads are taken as $\bar{\theta}$, the approximately circular intersections of the shower cones with the S-plane will all lie within an annular area of mean radius R, whose exact dimensions are readily determined. They depend on h as well as on $\bar{\Phi}$ and $\bar{\theta}$. The fractional areas of these rings lying inside the actual tray area were determined graphically for different values of h corresponding to the heights of the lead plates. Taking into account the "insensitive area" of the lead strips between the counters in the S-tray, the values of ρ are obtained from the above ratios simply by multiplying with an "efficiency" factor of 0.6.

APPENDIX II

(1) The Transition Effect

The change in the number of relativistic particles with absorber thickness is due to the following processes:

(a) Absorption of particles reaching the end of their range. In Sec. III.2 the approximate expression (1) was given for the number of particles stopped in an absorber thickness x, and "absorption coefficients" of 45 g/cm² and 500 g/cm² were found for the two groups of different penetration. Evidently, only the absorption of the first group will be of significance within the comparatively small range of thicknesses (less than 100 g/cm²) involved in the transition effect in the chamber. Thus, it will be assumed that "a-particles," whose number is $N_a=aN_s$ according to Sec. III.2, will be attenuated exponentially with an absorption length of 45 g/cm², while the $N_b=(1-a)N_s=bN_s$ "b-particles" will traverse the chamber without losses.

(b) All charged penetrating secondaries reproduce cascade particles with an interaction mean free path $\Lambda_s=250$ g/cm², and an average multiplicity of $\sigma=1.5$ penetrating particles per event.

(c) Neutrons will initiate secondary events with the same mean free path and average multiplicity. Their number is assumed to be equal to that of the protons: $N_n=N_p$. At the shower origin one can further set $N_n=r_pN_s$.

Neglecting third generation particles, one has for the number N of charged cascade particles at depth ξ

$$dN(\xi)=(\sigma-1)N_a(\xi)d\xi/\Lambda_s+(\sigma-1)N_b(\xi)d\xi/\Lambda_s+\sigma N_n d\xi/\Lambda_s. \quad (8)$$

Since ionization losses have been assumed to be negligible for the "b-particles," one has, for not too large absorber thicknesses, $N_n=rN_b$, with the constant $r=r_p/(1-a)$. Furthermore, from (a)

$$N_a=aN_se^{-\xi/x_0}, \quad (9)$$

and since $N(\xi)=N_a(\xi)+N_b(\xi)$, Eq. (8) can be rewritten in the form

$$dN_b(\xi)-[(r+1)\sigma-1]N_b(\xi)d\xi/\Lambda_s = aN_se^{-\xi/x_0}[1/x_0+(\sigma-1)/\Lambda_s]d\xi. \quad (10)$$

The integration of Eq. (10) can be performed; writing $q=(r+1)$, $\mu_0=1/x_0$, $\mu_s=1/\Lambda_s$, and $k=[\mu_0+(\sigma-1)\mu_s]/[\mu_0+(q\sigma-1)\mu_s]$ one has

$$N_b(\xi)=N_s\{[1+a(k-1)]e^{(q\sigma-1)\mu_s\xi}-ake^{-\mu_0\xi}\}, \quad (11)$$

from which one gets for the total number of charged particles under an absorber ξ

$$N(\xi)=N_s\{[1+a(k-1)]e^{(q\sigma-1)\mu_s\xi}-a(k-1)e^{-\mu_0\xi}\}. \quad (12)$$

Substituting the numerical values derived above, one finds for small showers ($N_s\leqslant 2$)

$$N(\xi)=N_s\{0.92e^{0.0071\xi}+0.08e^{-0.022\xi}\}, \quad (13)$$

while for large showers, $N_s>2$, the corresponding expression is

$$N(\xi)=N_s\{0.93e^{0.0062\xi}+0.07e^{-0.022\xi}\}. \quad (14)$$

One notices that in both cases $dN/d\xi>0$. The equations are, of course, applicable only as a rough approximation for thicknesses small compared with both the absorption length of the "penetrating group" and the interaction mean free path of the secondaries.

(2) Evaluation of the Triggering Probability $W(\varrho,N)$

In principle it is now possible to compute the probabilities W from Eqs. (7) and (13) or (14) for all initial multiplicites N_s and shower locations. However, as very large showers are infrequent, this procedure would leave one with insufficient statistics for these categories. Moreover, it is evident that for large showers, W becomes rather insensitive to a variation of N_s. The numerical computations were therefore carried out for the three groups of events listed in Table III: $N_s\leqslant 2$, $N_s=3$, and $N_s\geqslant 4$.

The first step was to determine for each group the average number of penetrating secondaries $\bar{N}_s$. The result was $\bar{N}_s=1.85$ for the smallest and $\bar{N}_s=4.35$ for the largest showers. With these figures, the probabilities $W(\rho, N)$ can now be computed for each multiplicity group and for each height of production, h, corresponding to a lead plate. The transition effect was calculated from Eq. (13) for the first group, ($N_s\leqslant 2$), and from Eq. (14) for the other two. The results are summarized in Table IV. It is remarkable that under the conditions of this experiment, the triggering probabilities vary only slightly with the height of production of the primary event in the chamber. The dependence on the number of secondaries is much more marked.